LASER INTERFEROMETER GRAVITATIONAL WAVE OBSERVATORY
- LIGO -
CALIFORNIA INSTITUTE OF TECHNOLOGY
MASSACHUSETTS INSTITUTE OF TECHNOLOGY

Technical Note	**LIGO-T060178-00-D**	2006/07/24
Estimate of the Beam Jitter at the Output Mode Cleaner		
V. Mandic		

This is an internal working
note of the LIGO project

California Institute of Technology
LIGO Project, MS 18-34
Pasadena, CA 91125
Phone (626) 395-2129
Fax (626) 304-9834
E-mail: info@ligo.caltech.edu

Massachusetts Institute of Technology
LIGO Project, Room NW17-161
Cambridge, MA 02139
Phone (617) 253-4824
Fax (617) 253-7014
E-mail: info@ligo.mit.edu

LIGO Hanford Observatory
Route 10, Mile Marker 2
Richland, WA 99352
Phone (509) 372-8106
Fax (509) 372-8137
E-mail: info@ligo.caltech.edu

LIGO Livingston Observatory
19100 LIGO Lane
Livingston, LA 70754
Phone (225) 686-3100
Fax (225) 686-7189
E-mail: info@ligo.caltech.edu

WWW: http://www.ligo.caltech.edu/

1 Outline

This note summarizes a calculation of the beam jitter noise at the output mode cleaner (OMC). We would like to examine the following questions:

1. What is the level of the strain-equivalent noise produced by the beam jitter at the OMC waist?
2. Is there a requirement on the bandwidth of the PZT-mirror system upstream from the OMC, due to the beam jitter?
3. What is the contribution of the beam-reducing telescope to the beam jitter, and should it be reduced?
4. Should the OMC be suspended, and how much? Is there a preference regarding the chamber (BSC, 1-stage HAM etc)?

To answer these, we need the following pieces:

- Determine the angular motion of the core optics (ETMs and ITMs are the most relevant). Propagate the corresponding beam jitter to the OMC waist.
- Determine the motion of the beam-reducing telescope (displacement and angle). Propagate the corresponding beam jitter to the OMC waist.
- Convert the beam jitter (displacement and angle) at the OMC waist into power fluctuations at the OMC.
- Convert the power fluctuations at the OMC into strain-equivalent noise and compare it with the SRD curve.
- Investigate effects of the PZT system.
- Compare the beam jitter at the OMC waist with the displacement noise at the top of a chamber stack (BSC, 1-stage HAM etc). Should the OMC be suspended? Should the beam-reducing telescope be suspended?

2 Setup

Figure 1 shows the setup used in this calculation. It defines several lengths and mirrors (listed in the Table 1). The beam jitter due to the angular motion of the core optics is first estimated at the input of the beam-reducing telescope (mirror A). Similarly, the beam jitter due to the motion of the beam reducing telescope is also assumed to be at the input of the telescope. These contributions are then propagated to the OMC waist using the following ABCD propagators:

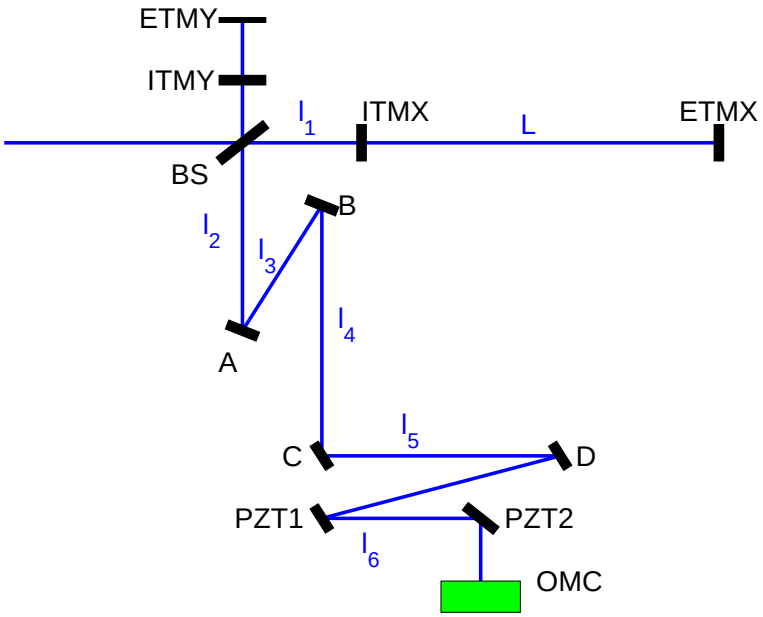

Figure 1: Setup. Mirrors A and B define the beam-reducing telescope, currently installed in HAM4 (no suspension). Mirrors C and D define the OMC telescope. Distance l_6 is the total distance from mirror D to OMC waist.

Parameter	Value	Note
l_1	4.6 m	Rough Estimate, from M. Smith
l_2	4.5 m	Rough Estimate, from M. Smith
l_3	1.3 m	Design, M. Smith
l_4	16.3 m	Rough Estimate, from M. Smith
l_5	0.48 m	Design, M. Smith
l_6	0.8 m	Rough Estimate, S. Waldman
R_A	3.05 m	Design, M. Smith
R_B	0.38 m	Design, M. Smith
R_C	0.75 m	Design, M. Smith
R_D	0.18 m	Design, M. Smith
R_{ITM}	14 km	Average over several optics
R_{ETM}	8 km	Average over several optics
L	3995 m	

Table 1: Values of parameters defined in Figure 1.

- Beam-reducing telescope:

$$M_1 = \begin{pmatrix} 1 & 0 \\ -2/R_B & 1 \end{pmatrix} \begin{pmatrix} 1 & l_3 \\ 0 & 1 \end{pmatrix} \begin{pmatrix} 1 & 0 \\ -2/R_A & 1 \end{pmatrix}$$

- Propagator to OMC telescope:

$$M_2 = \begin{pmatrix} 1 & l_4 \\ 0 & 1 \end{pmatrix}$$

- OMC telescope:

$$M_3 = \begin{pmatrix} 1 & 0 \\ -2/R_D & 1 \end{pmatrix} \begin{pmatrix} 1 & l_5 \\ 0 & 1 \end{pmatrix} \begin{pmatrix} 1 & 0 \\ -2/R_C & 1 \end{pmatrix}$$

- Propagator to OMC waist:

$$M_4 = \begin{pmatrix} 1 & l_6 \\ 0 & 1 \end{pmatrix}$$

- Total:

$$M = M4 \times M3 \times M2 \times M1. \quad (1)$$

3 Contribution of the Core Optics

3.1 Angular Motion of Core Optics

The angular motion of the core optics is estimated using the calibrated spectrum of the WFS signals. In particular, we used the calibration of WFS1 from LLO (April 2006). This calibration gave $\sim 4 \times 10^5$ WFS1-counts per ETM-microradians (the difference between ETMX/ETMY and pitch/yaw was about 20%, so we use an average over the four cases here; we also ignore the contribution due to ITMs, which is significantly lower, especially in quadrature). Hence, we take WFS1 spectrum and divide it by this calibration factor (and by $\sqrt{2}$) to get the angular motion spectrum of ETMs. We assume ITMs and the BS have the same spectrum. The spectrum is shown in Figure 2.

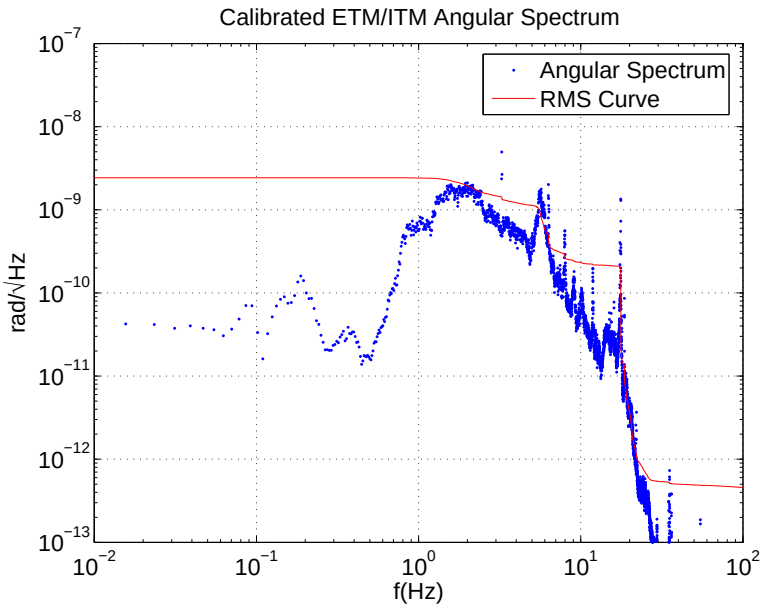

Figure 2: Angular spectrum of core optics.

3.2 ETM Contribution

We assume the IFO is in a "perfect" state, and then we tilt ETM by angle θ. The beam inside the cavity will move to the new cavity axis, defined by the two centers of mirror curvatures. It is straightforward to show that the beam will be tilted at an angle:

$$\alpha = \arctan \frac{R_{ETM} \sin\theta}{R_{ITM} + R_{ETM}\cos\theta - L} \approx 0.44\ \theta \tag{2}$$

and the position of the beam on the ITM is:

$$r_{ITM} = \frac{R_{ITM}\alpha}{\sqrt{1+\alpha^2}} \approx 0.44\ R_{ITM}\ \theta \tag{3}$$

This is then propagated using the ray matrix algebra to the first mirror (A) of the beam-reducing telescope.

$$\begin{pmatrix} r \\ r' \end{pmatrix}_A = \begin{pmatrix} 1 & l_1 + l_2 \\ 0 & 1 \end{pmatrix} \begin{pmatrix} 0.44\ R_{ITM}\ \theta \\ 0.44\ \theta \end{pmatrix}$$

3.3 ITM Contribution

We do similar analysis tilting ITM by angle θ. Again, the beam inside the cavity will move to the new cavity axis, defined by the two centers of mirror curvatures. The beam angle is given by:

$$\alpha = \arctan \frac{-R_{ITM} \sin\theta}{L - R_{ETM} - R_{ITM}\cos\theta} \approx 0.78\ \theta \tag{4}$$

and the position of the beam on the ITM is:

$$r_{ITM} = -\frac{R_{ITM}\alpha}{\sqrt{1+\alpha^2}} + R_{ITM}\sin\theta \approx 0.22\ R_{ITM}\ \theta \tag{5}$$

This is then propagated using the ray matrix algebra to the first mirror (A) of the beam-reducing telescope.

$$\begin{pmatrix} r \\ r' \end{pmatrix}_A = \begin{pmatrix} 1 & l_1 + l_2 \\ 0 & 1 \end{pmatrix} \begin{pmatrix} 0.22\ R_{ITM}\ \theta \\ 0.78\ \theta \end{pmatrix}$$

3.4 Beam Splitter Contribution

If the BS is tilted by θ, the beam coming from ITMX will scatter at the angle $\theta + \pi/4$, and the beam is then propagated by the distance between the BS and the first mirror (A) of the beam-reducing telescope.

$$\begin{pmatrix} r \\ r' \end{pmatrix}_A = \begin{pmatrix} 1 & l_2 \\ 0 & 1 \end{pmatrix} \begin{pmatrix} 0 \\ 2\theta \end{pmatrix}$$

There are other contributions, from the Y-arm, but they seem to be comparable in size, and much smaller than the ETM or ITM contributions.

4 Contribution of the Beam-Reducing Telescope

4.1 Estimate of Ground Noise

We use accelerometer signals to estimate the motion above 5 Hz (calibration 6e-6 m/cnt, with a double pole at 0 Hz). Below 5 Hz, we use the seismometer signals (STS2 at LLO, calibration 4.4e-10 m/cnt with a pole at 0 Hz). The accelerometers and seismometers readings agree around 5 Hz. The ground noise estimate obtained in this way is shown in the Figure 3.

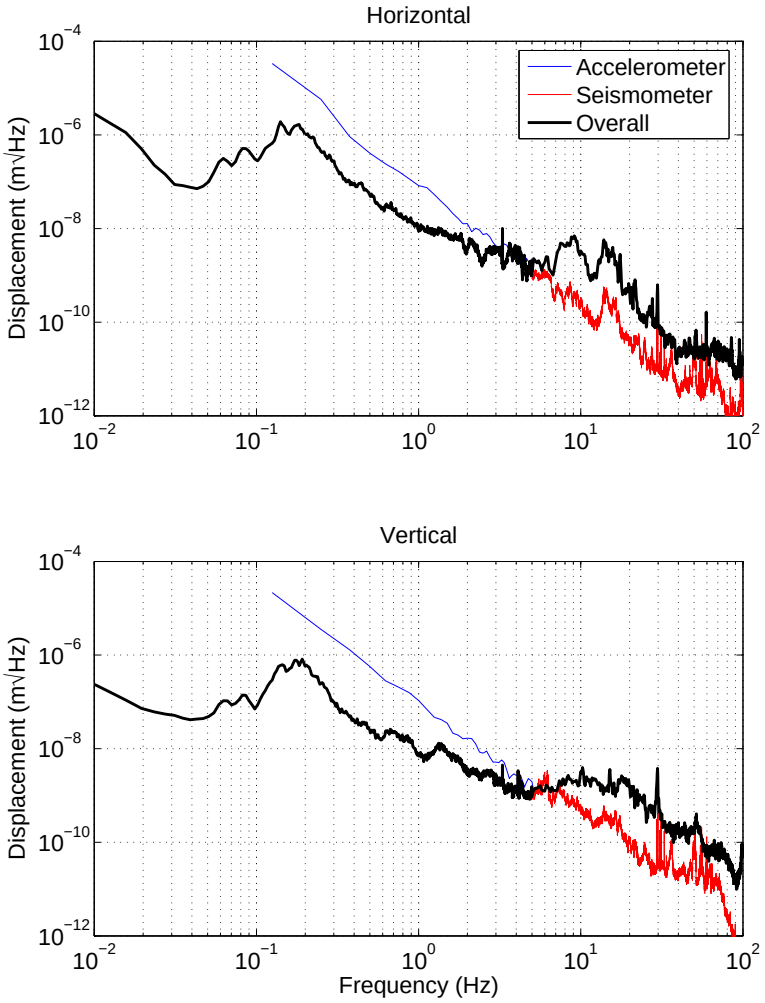

Figure 3: Estimate of the ground noise.

4.2 Motion of the Beam-Reducing Telescope

The beam reducing telescope is mounted on HAM4, with no suspension. Hence, its motion with respect to the beam is the same as the motion of the top of the HAM stack. Figure 4 shows the spectra for different degrees of freedom at the top of the HAM stack. These are

based on the ground noise shown in Figure 3 and the HAM stack model. For the angular ground noise, we use the ground displacement noise divided by 10 (suggested by Rana). For this Figure, the x-axis is along the beam, and y and z are the transverse horizontal and vertical directions (θ_i is the rotation angle around axis i). We assume that this noise is at the input of the beam-reducing telescope.

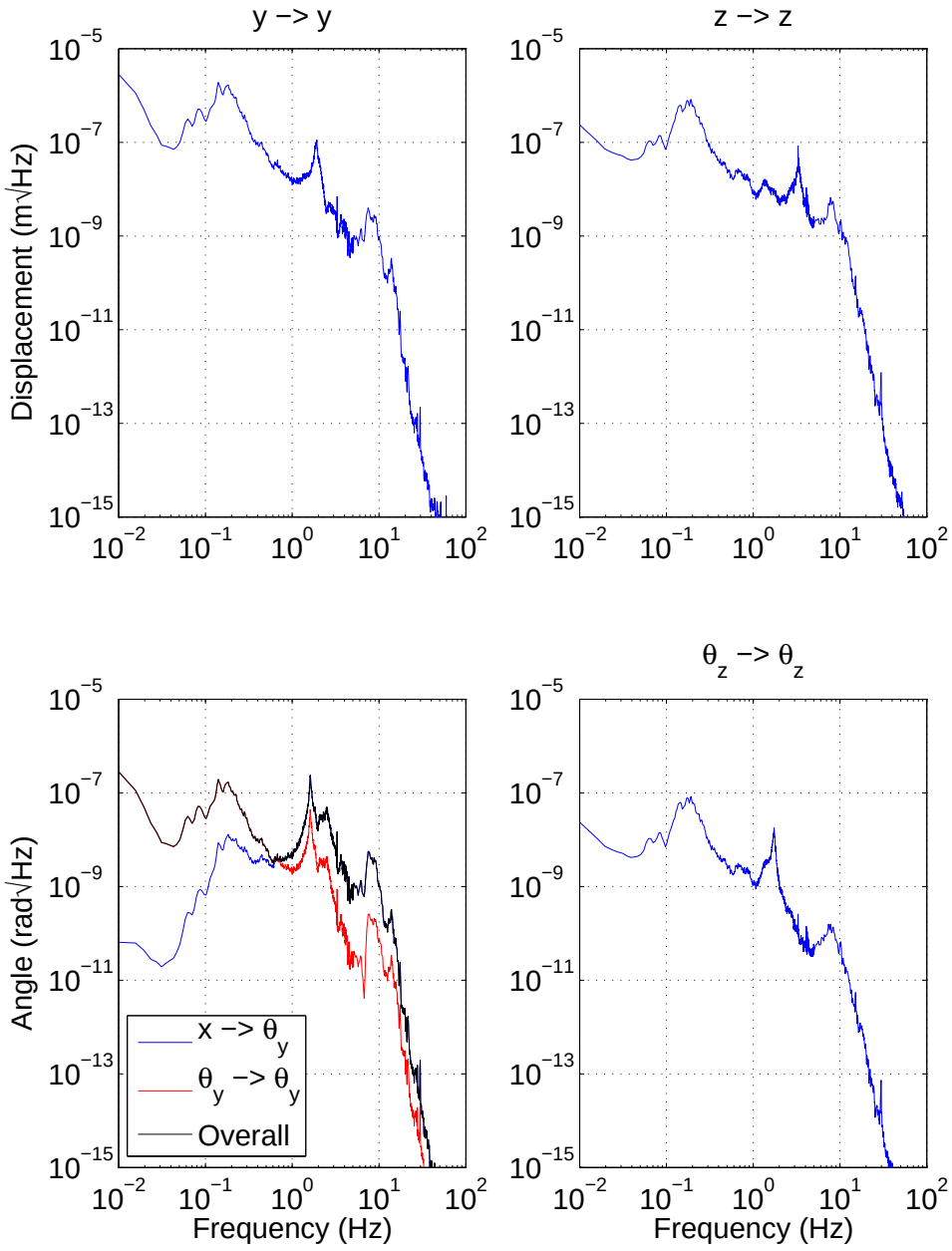

Figure 4: Estimate of the noise at the top of HAM stack (i.e. beam-reducing telescope noise). See text for details.

5 Beam Displacement and Tilt Noise at the OMC

Previous Sections discussed the various sources of the beam jitter, and how they should be propagated to the OMC waist.

Figure 5 shows the different contributions to the beam displacement noise. At frequencies above ~ 0.3 Hz the motion of the core optics dominates, while below 0.3 Hz the dominant contribution is due to the beam-reducing telescope. The (quadrature) sum of the contributions is significantly larger than the expected motion of the OMC itself, if it were installed on ALIGO BSC stack or 1-stage HAM stack (with no suspension). This plot does not take into account effects of the PZT system upstream of the OMC.

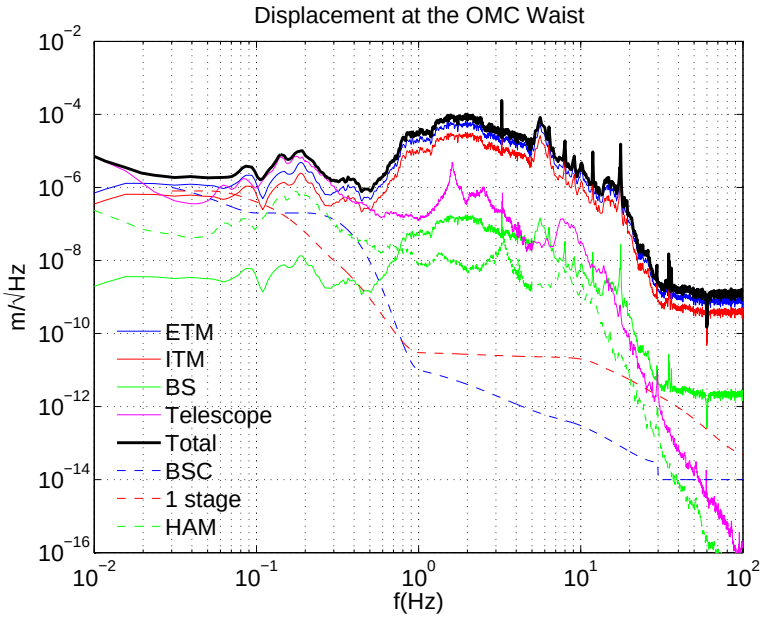

Figure 5: Estimate of the beam displacement noise at the OMC waist. Different contributions are shown, and are compared with the expected displacement spectrum at the top of different stacks.

Figure 6 shows similar contributions to the beam tilt noise at the OMC waist. Again, the effect of the PZT system is not included.

Figure 7 shows the total beam jitter (displacement and angle) with the corresponding RMS curves. We also show the impact of the PZT system, for which we assume $1/f$ open-loop-gain, with the unity gain frequency UGF=50 Hz. The PZT system is expected to significantly reduce the RMS, which is especially important for the displacement case, where the relevant scale is the beam waist of 0.4 mm. The PZT filtering does not change the conclusion that the beam jitter is expected to be significantly larger than the motion of the OMC if it were installed with no suspension on ALIGO BSC stack, or on 1-stage HAM stack.

Finally, we note that at frequencies above 30 Hz, the dominant contribution to the displace-

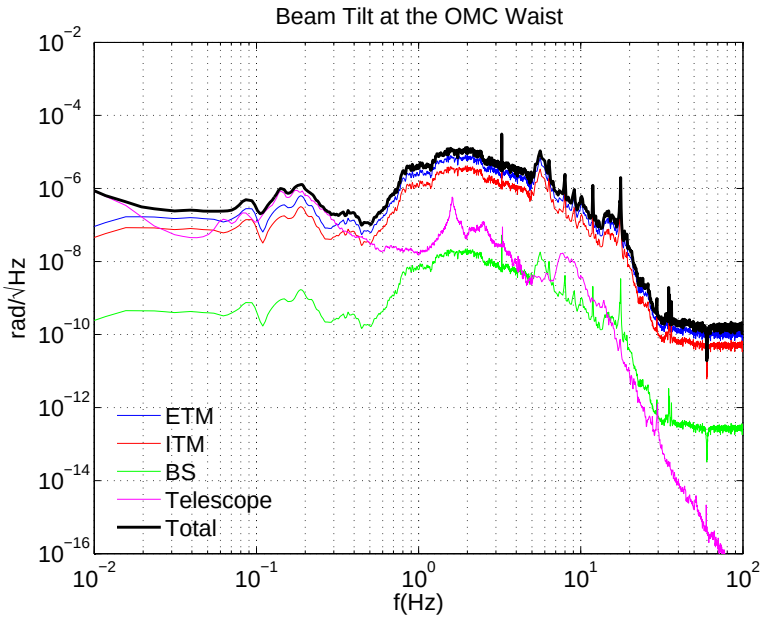

Figure 6: Estimate of the beam tilt noise at the OMC waist. Different contributions are shown.

ment of the beam is the angular motion of the core optics. This motion is estimated using the WFS spectrum, and above 30 Hz the estimate is probably not reliable. Figure 8 shows how the spectrum would look like if we simply extrapolate it based in the 20-30 Hz region. In this case, the beam jitter would be smaller than the motion at the top of the ALIGO BSC stack (or of the 1-Stage HAM stack) above ~ 60 Hz. So, in this case it would be good to suspend the OMC, and according to Figure 8, $1/f^2$ with resonant frequency at ~ 5 Hz, should be sufficient for either of the two chambers.

6 Estimating Power Fluctuation in OMC

In the previous Section we estimated the displacement and angle jitter of the beam at the OMC waist. We now want to estimate the corresponding power fluctuation of the 00-mode in the OMC. For this, we follow the paper by Dana Anderson (Appl. Optics 23, 2944 (1984)) and expand to second order. Of the four effects investigated in the Anderson paper, two seem relevant (beam displacement and beam tilt). The two mode-matching effects (beam waist size and position) seem to be less of a concern - waist size does not seem to change by the effects investigated here, and the waist position introduces power fluctuation that goes as the fourth power of the beam tilt angle.

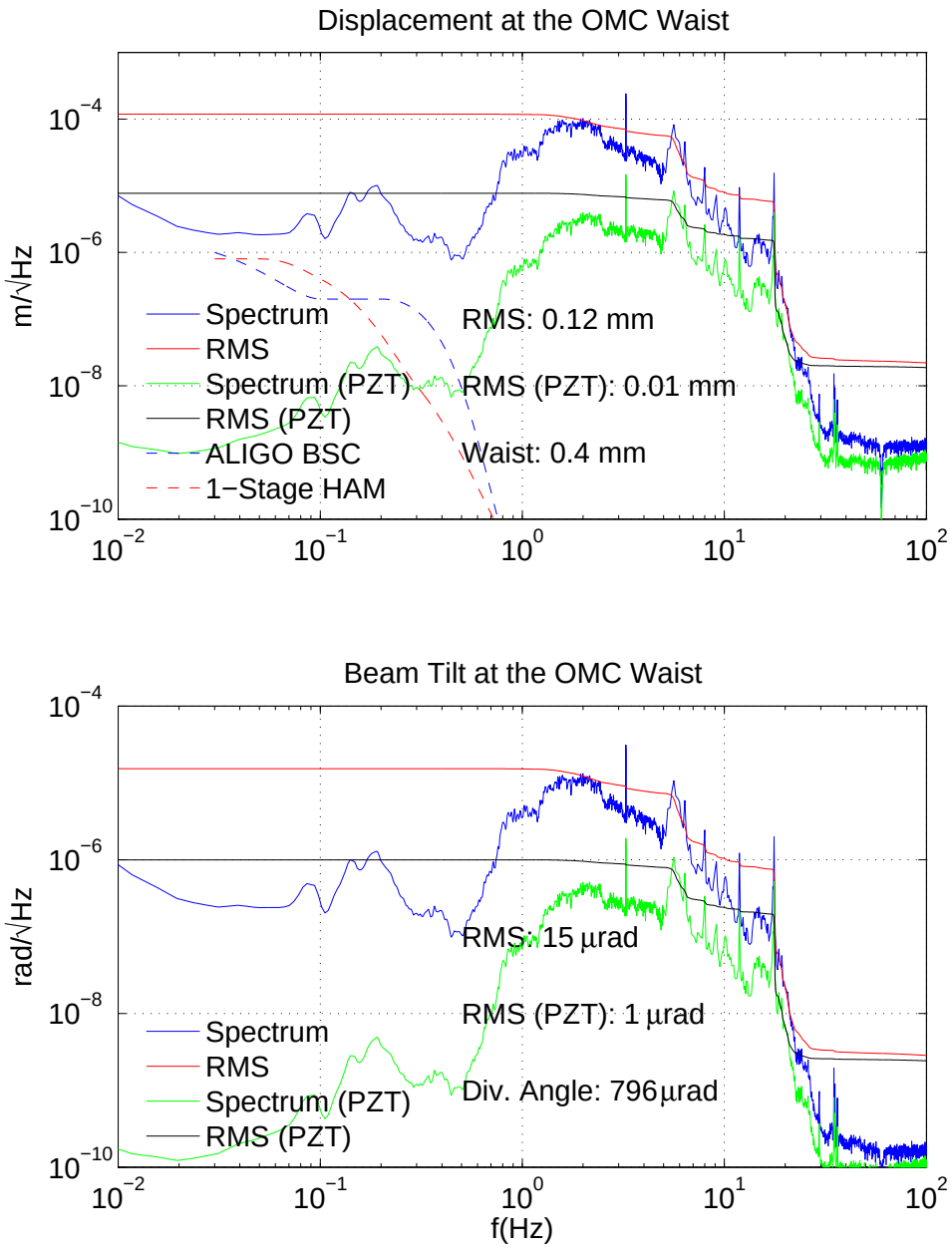

Figure 7: Effect of the PZTs on the beam jitter at the OMC waist.

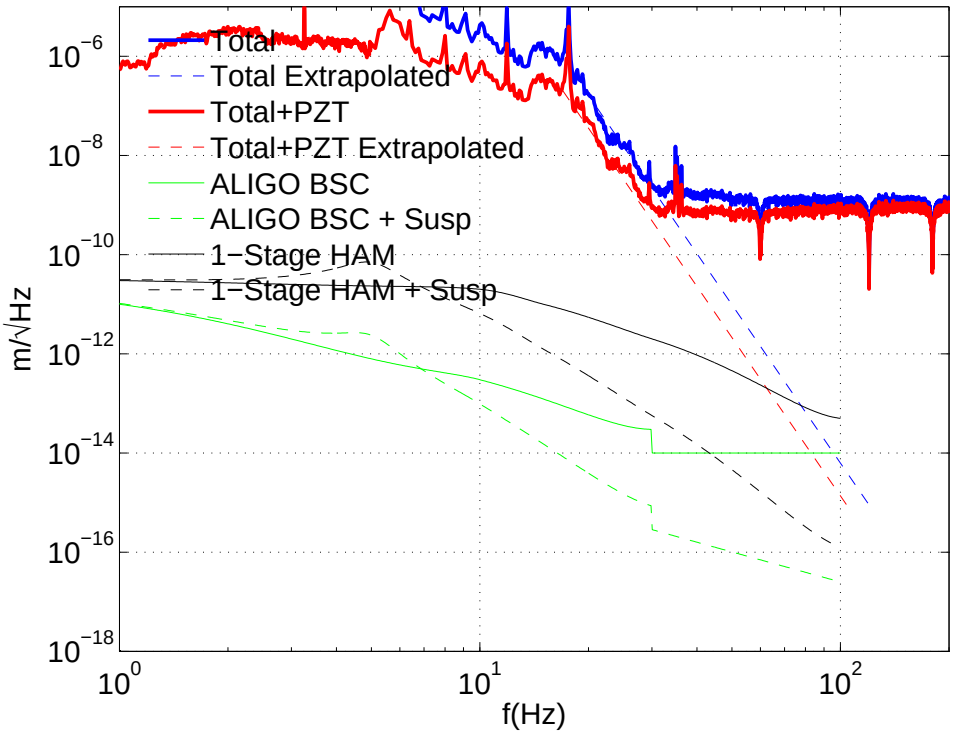

Figure 8: Displacement noise: Extrapolating total beam jitter from 20-30 Hz to above 30 Hz. Also shown is the effect of the PZT system. Also shown are the displacement spectra at the top of the ALIGO BSC and 1-stage HAM stacks. The effect of the OMC suspension is also shown. Note: Virginio S. has provided a calculation of the HAMSAS performance up to 35 Hz - it agrees well with the ALIGO BSC requirement curve, shown in this Figure.

6.1 Beam Displacement

We start with a pure 00-mode travelling in the z-direction. The amplitude at distance x from the z-axis is given by:

$$\psi(x) = A\left(\frac{2}{\pi x_0^2}\right)^{1/4} \exp\left[-\left(\frac{x}{x_0}\right)^2\right], \tag{6}$$

where x_0 is the beam waist. Displacing the beam by a implies:

$$\begin{aligned}
\psi(x-a) &= A\left(\frac{2}{\pi x_0^2}\right)^{1/4} \exp\left[-\left(\frac{x-a}{x_0}\right)^2\right] \\
&= A\left(\frac{2}{\pi x_0^2}\right)^{1/4} \left[\exp\left[-\left(\frac{x}{x_0}\right)^2\right] + \frac{2xa}{x_0^2}\exp\left[-\left(\frac{x}{x_0}\right)^2\right]\right. \\
&- \left.\frac{a^2}{x_0^2}\exp\left[-\left(\frac{x}{x_0}\right)^2\right] + \frac{2a^2x^2}{x_0^4}\exp\left[-\left(\frac{x}{x_0}\right)^2\right] + ...\right] \\
&= \left(1 - \frac{a^2}{x_0^2}\right)\psi(x) + 01 \text{ Term} + ...
\end{aligned} \tag{7}$$

6.2 Beam Tilt

If the input beam enters the cavity at an angle α, it will cause a phase shift at the waist that is dependent on the transverse dimension:

$$\begin{aligned}
\psi(x) &= U_0(x)\exp(\frac{2\pi i\alpha x}{\lambda}) \\
&= U_0(x)\left(1 + \frac{2\pi i\alpha x}{\lambda} - \frac{(2\pi\alpha x)^2}{\lambda^2}\right) \\
&= \left(1 - \frac{2\alpha^2}{\theta_D^2}\right)U_0(x) + \frac{\pi i\alpha x_0}{\lambda}U_1(x) - \frac{\pi^2\alpha^2x_0^2}{\lambda^2}U_2(x) + ...
\end{aligned} \tag{8}$$

Here, $U_i(x)$ is the i^{th} Hermite polynomial, and $\theta_D = \lambda/(\pi x_0)$ is the divergence angle of the OMC cavity.

6.3 Power Fluctuation

Pulling these together, we get:

$$\begin{aligned} P(x,a,\alpha) &= |\psi(x,a,\alpha)|^2 = |\psi(x)\ (1-a^2/x_0^2)\ (1-2\alpha^2/\theta_D^2)|^2 \\ &= P(x)\left(1-\frac{2a^2}{x_0^2}-\frac{4\alpha^2}{\theta_D^2}\right) \end{aligned} \tag{9}$$

The last equation allows us to calculate the power fluctuation due to displacement and tilt fluctuations at the OMC waist. However, our estimates of the beam jitter are frequency dependent (i.e. a and α are power spectra). It is, therefore, non-trivial to estimate a^2 and α^2. We will consider two approaches:

- Define $a^2(f) \equiv a(f) \times$ RMS$(a(f))$. With this definition, $a^2(f)$ has the same spectral shape as $a(f)$, and it is scaled so that RMS$(a^2(f))$ = RMS$^2(a(f))$. We do the same for α^2.
- Define $a^2(2f) \equiv a(f) \times a(f)$ - i.e. squaring the amplitude of a at frequency f gives the amplitude of a^2 at $2f$. This definition makes the spectrum of a^2 broader than that of a. We do the same for α^2.

With these assumptions, we calculate the power fluctuation at the OMC due to the beam displacement (second term in Equation 9) and due to the beam tilt (third term in Equation 9). These are shown in Figure 9. The displacement term seems to dominate over the tilt term. Moreover, the PZT filter discussed in the previous Section ($1/f$ with UGF=50 Hz) significantly reduces the power fluctuations.

7 Estimating Strain-Equivalent Noise

The last step of this calculation is to convert the power fluctuations at the OMC into strain-equivalent noise. To do this, we start with the following expression for the power at the AS port that holds for the simple Michelson:

$$P_{AS} = P_{BS}\ \sin^2\Phi_- \tag{10}$$

$$\Phi_- = \frac{2\pi N_{arm} L_-}{\lambda}, \tag{11}$$

where P_{BS} is the power at the beam splitter, $N_{arm} = 137$ is the arm cavity gain, L_- is the difference in arm lengths, and λ is the beam wavelength. Assuming DC readout, we pick the

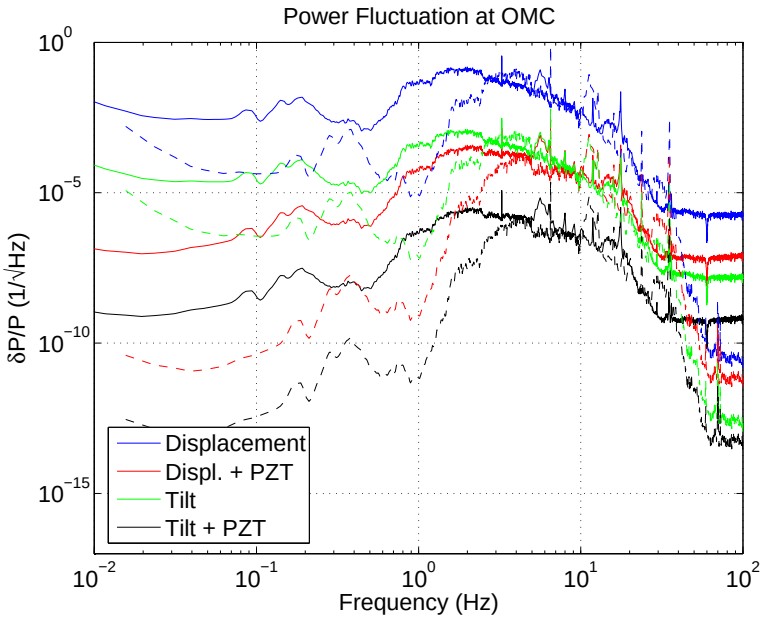

Figure 9: Power fluctuation at the OMC. The solid curves were calculated using definition $a^2(f) \equiv a(f) \times \mathrm{RMS}(a(f))$ (similar for α^2), and the dashed were calculated using definition $a^2(2f) \equiv a(f) \times a(f)$ (similar for α). See text for details.

operational point with $L_- = 10$ pm (suggested by Rana). Then we can write:

$$\frac{dP_{AS}}{dL_-} = P_{BS} \frac{2\pi N_{arm}}{\lambda} \sin \frac{2\pi N_{arm} 2L_-}{\lambda} \tag{12}$$

$$\delta P_{AS} = \epsilon(f) P_{AS} = \left(\frac{2a^2(f)}{x_0^2} + \frac{4\alpha^2(f)}{\theta_D^2} \right) P_{AS} \tag{13}$$

$$\delta L_- = \frac{\delta P_{AS}}{dP_{AS}/dL_-} = \frac{\lambda \epsilon(f)}{4\pi N_{arm}} \tan \frac{2\pi N_{arm} L_-}{\lambda} \tag{14}$$

The last equation relates the power fluctuations estimated in the previous Section to the fluctuations in the arm length. It is now straightforward to calculate the strain-equivalent noise, given the beam displacement $a(f)$ and beam tilt $\alpha(f)$ at the OMC waist.

Figure 10 shows the strain-equivalent noise spectrum (with and without the PZT system) for the case when the "squared" spectra are defined as $a^2(f) \equiv a(f) \times \mathrm{RMS}(a(f))$ (and similar for α^2). They are compared to the SRD curve scaled down by a factor of 3.

Figure 11 shows a similar plot for the definition $a^2(2f) \equiv a(f) \times a(f)$ (and similar for α^2).

8 Comments and Conclusions

We summarize several conclusions of this analysis:

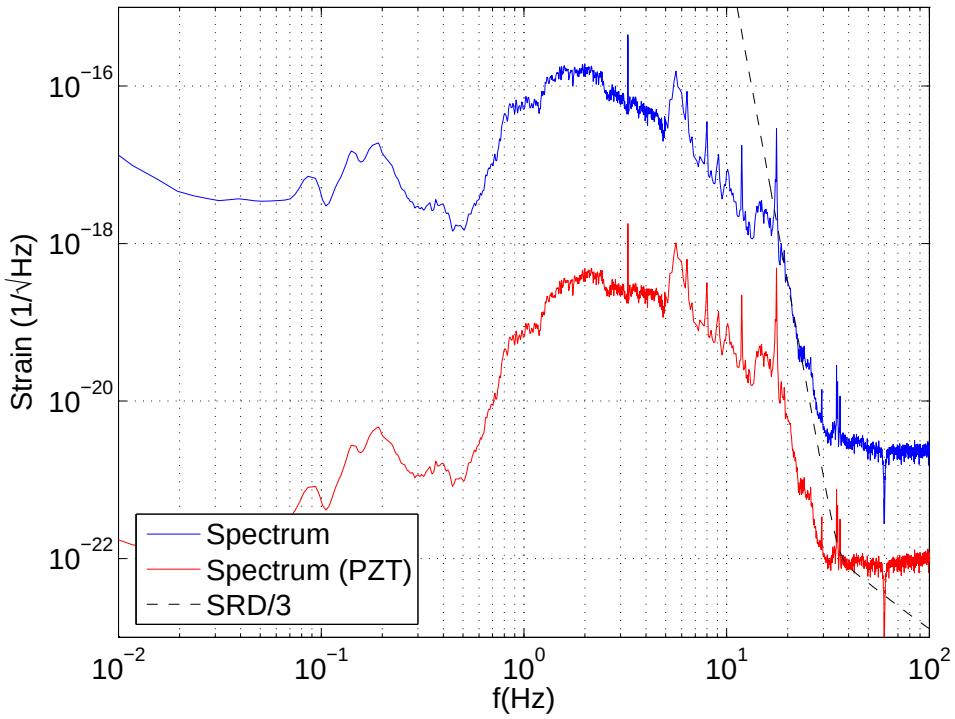

Figure 10: Strain-equivalent noise spectrum, for the definition $a^2(f) \equiv a(f) \times \mathrm{RMS}(a(f))$ (and similar for α^2). Note that the SRD curve is scaled down by a factor of 3. The difference between the blue and red curve is due to the PZT filter.

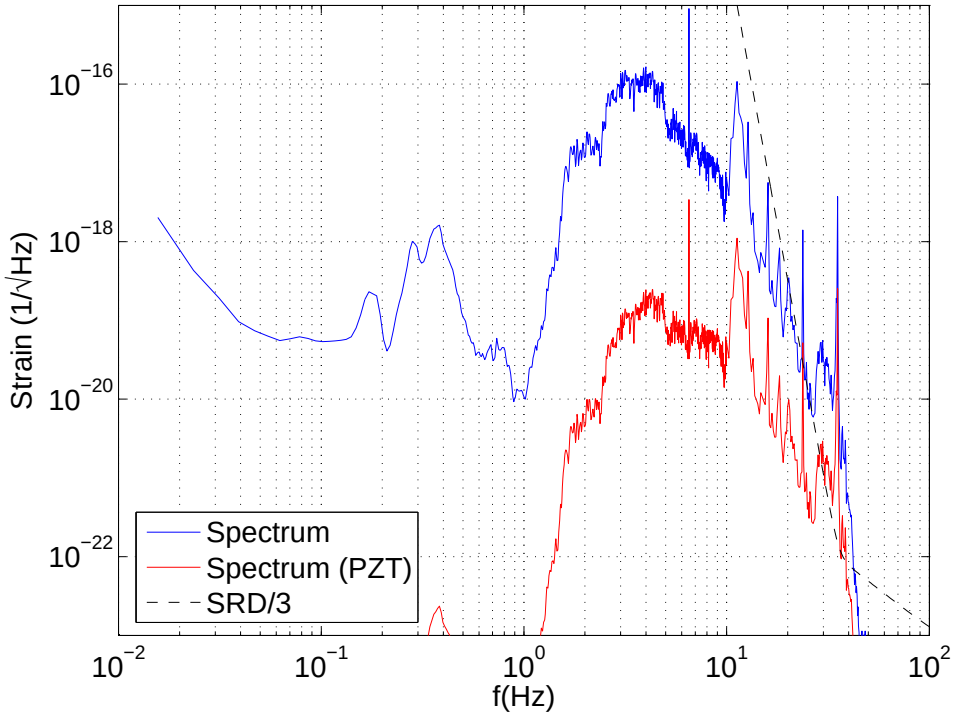

Figure 11: Strain-equivalent noise spectrum, for the definition $a^2(2f) \equiv a(f) \times a(f)$ (and similar for α^2). Note that the SRD curve is scaled down by a factor of 3. The difference between the blue and red curve is due to the PZT filter.

- The strain-equivalent noise due to the beam jitter at the OMC waist, shown in Figures 10 and 11, appears significant above $\sim$ 15 Hz. The PZT filter, for which we assumed $1/f$ open loop gain, with UGF=50 Hz, significantly improves the situation, but more gain would probably be appropriate. Note that the flat part of the spectrum above $\sim$ 30 Hz in Figure 10 comes from the WFS spectrum, and it is probably not a faithful representation of the angular motion of the core optics. Also, the dominant contribution to the strain-equivalent noise is the displacement of the beam (not the beam tilt), as shown in Figure 9.

- The beam jitter is dominated by the angular motion of the core optics above 0.3 Hz. Below 0.3 Hz, the beam-reducing telescope becomes important. Hence, it does not appear necessary to suspend the beam-reducing telescope.

- The motion of the OMC itself, if it were installed directly on the ALIGO BSC stack, or on the 1-stage HAM stack, would be significantly smaller than the beam jitter at most frequencies. This is shown in the Figures 5, 6 and 7. However, the beam jitter estimate at high frequencies is dominated by the angular motion of the optics - above 30 Hz our estimate of this motion, which is based on the WFS spectrum, is probably not reliable. Hence, it is possible that above $\sim$ 60 Hz the motion of the OMC will become comparable to (or larger than) the angular motion of the optics, as shown in Figure 8. In this case, suspending the OMC with $\sim$ 5 Hz resonant frequency (and $1/f^2$ noise suppression at higher frequencies) seems sufficient to bring the OMC motion below the beam jitter level, for either of the two chambers. Note, however, that in terms of the strain-equivalent noise this does not seem to be an issue.